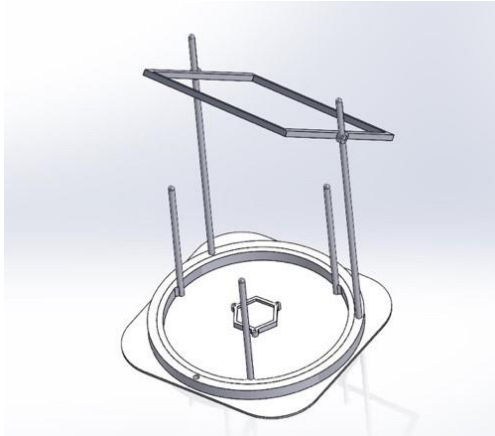


Prudent Landers: Fresnel Assisted Sintering Technology (F.A.S.T)



Colorado School of Mines

Team Members:

Ethan Adam – Mechanical Eng. (Undergraduate) - Team Leader
Harrison Fugate – Mechanical Eng. (Undergraduate) - CFO
Justus Quint von Lengerke – Mechanical Eng. (Undergraduate) - Communications Lead
Cora Perkins – Mechanical Eng. (Undergraduate)
Casey Hubbs – Mechanical Eng. (Undergraduate)
Max Pizzimenti – Mechanical Eng. (Undergraduate)
Noah Pruitt – Mechanical Eng. (Undergraduate)
Alex Fisher – Electrical Eng. (Undergraduate)
Madeleine Nightengale-Luhan – Electrical Eng. (Undergraduate)
Aiden Semet – Electrical Eng. (Undergraduate)

Advisors:

Chief Technical Advisor - Dr. Angel Abbud-Madrid, Dir. of Space Resources Program at CSM
Technical Advisor – David Purcell, Ph.D. Student in Space Resources Program at CSM
Faculty Advisor – Prof. Mark Florida, Capstone Design Advisor at CSM

Quad Chart

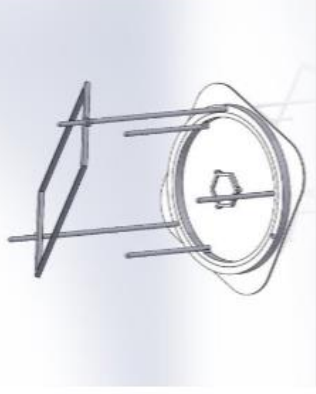
Colorado School of Mines – Prudent Landers



Major Objectives & Technical Approach

- Objectives
 - Reduction / mitigation of erosion (cratering) and ejecta during descent, landing, and ascent
- Technical Approach
 - Create a landing pad through sintering of regolith using a Fresnel Lens (focused sunlight)
 - Sinter regolith into hexagonal tiles to form the landing pad
 - Build the landing pad utilizing an LTV vehicle for tile placement and a 100 W laser rover for sintered grouting

Image/Graphic:



Key Design Details & Innovations of the Concept

- Design Details
 - Fresnel Lens rotating on a circular track to constantly follow the sun using photodiodes and FSS's (Fine Sun Sensors)
 - 3D printing bed concept for optimized regolith sintering depth
 - Power requirement of 931.65 Watts
- Innovations
 - Fresnel Lens design and track for lunar implementation and regolith brick development
 - Landing pad design using hexagonal design

Summary of Schedule & Costs for the proposed solution's path to adoption

- Schedule
 - Phase A: concept and technology development, can be completed within this fiscal year assuming concept studies have already been performed via this team's proposal
 - Phase B: Preliminary Design, will take the project into 2025
 - Phase C: Final Design and Fabrication, is estimated to take a year into 2027
 - Phase D: System Assembly, Integration & Test, Launch will put the program ready for launch in 2027
- Costs
 - NASA Cost Estimation Toolkit estimated costs to be \$2,430,000 over mission lifetime
 - Launch costs are \$252,795, assuming a launch with Falcon Heavy

Table of Contents:

Table of Tables:	1
Table of Equations:	1
Problem Statement & Background	2
Project Description	2
Design Overview	2
Changes Made Since Proposal	3
Addressing Tile Grout	3
Addressing Testing in a Vacuum Environment	4
Addressing Lunar Operations	4
Addressing Solar Inclination Angle	5
Addressing Fresnel Lens Material	6
Innovative Technology	6
Engineering Analysis	6
Fresnel Lens	6
Heat Transfer Calculations	7
Electrical Subsystem	8
Sintering Bed	9
Verification and Validation	9
Conclusion	10
Path-To-Flight Timeline	10
Cost Estimation	11
I. Appendix One – Heat Transfer Calculations:	13
II. Appendix Two- References	15

Table of Figures:

Figure 1: Final Design Assembly..... 3
Figure 2: Snell's Law (input/output angles) 5
Figure 3: Pareto Front Relating Lens Mass to Negative Lens Power Output..... 7
Figure 4: Simulation Graph for Temperature vs. Time 8
Figure:5 Pareto Front Relating Lens Mass to Negative Lens Power Output..... 9
Figure:6 Testing of Fresnel Lens 10
Figure:7 Path-to-Flight Timeline11
Figure:8 Project Cost Timeline 12
Figure:9 Source Code for Heat Transfer Calculations 14

Table of Tables:

Table 1: Estimated Power Consumption of Required Components [ES3]-[ES5]..... 8

Table of Equations:

Equation 1: Transmissivity of Fresnel Lens5
Equation 2: Temperature at various times and depths7
Equation 3: Irradiation/Solar Flux (constant)13
Equation 4: Thermal Conductivity of Regolith13
Equation 5: Density of Regolith (constant)13
Equation 6: Volumetric Heat Capacity of Regolith13
Equation 7: Alpha Ratio.....13

Problem Statement & Background

Our team chose to focus on reducing Plume Surface Interaction (PSI) during the ascent, descent, and landing of human landing systems on the lunar surface. Through the use of Fresnel Assisted Sintering Technology (FAST) our solution utilizes a Fresnel lens to sinter lunar regolith into hexagonal shaped bricks to create a stable landing pad for future lunar landers. The sustainable, low power, and modular nature of our solution allows for the creation and maintenance of landing pads of varying sizes for future lunar missions.

Lunar PSI is a massive issue facing future lunar missions. Researching lunar PSI particularly in mitigating ejecta during ascent, descent, and landing, is crucial for successful spacecraft operations on the Moon. Understanding PSI, from basic surface impingement to chemical reactions, helps predict and manage the effects of rocket exhaust interacting with the lunar surface. This knowledge is essential for designing spacecraft with effective thermal protection systems to handle the heat generated during these phases and to ensure the safety of scientific instruments aboard. Additionally, understanding PSI aids in optimizing engine performance, ensuring efficient propulsion during lunar landings and takeoffs. By studying PSI, engineers can develop strategies to minimize potential damage to both the lunar environment and sensitive scientific instruments while ensuring the success of spacecraft missions.

The PSI challenge addressed pertains to mitigating ejecta during ascent, descent, and landing. Using a Fresnel lens, the lunar regolith undergoes sintering to form hexagonal bricks, creating a stable landing pad for the lunar lander. This not only facilitates proper landings by creating a stable and flat landing surface while also prevents the expulsion of lunar regolith. The sintered regolith composition minimizes the risk of regolith being scattered, as the solidified structure prevents loose grains from dispersing. The choice of the Fresnel lens laser solution stems from its unique design, rarity in lunar missions, cost-effectiveness, and ease of use during testing. The resulting sintered regolith bricks offer stability and durability for future landings. Implementing the Fresnel lens on the moon carries minimal risk, with upright technology readiness due to the accessibility and straightforward manufacturing of its components with appropriate equipment and environment.

Project Description

Design Overview

The FAST proposed solution is a device capable of sintering lunar regolith into hexagonal tiles by utilizing an automated rotating Fresnel lens that will track the sun's position in relation to the lunar surface and a motorized hexagonal bed to contain and shape the regolith during sintering. The angling and position of both the Fresnel lens and the regolith bed are automated to always ensure proper positioning of the focal point of the lens. The hexagonal tiles created by the device can be arranged and placed via an automated rover to create landing pads of varying sizes to significantly reduce any cratering and ejecta of lunar regolith during ascent, descent, and landing.

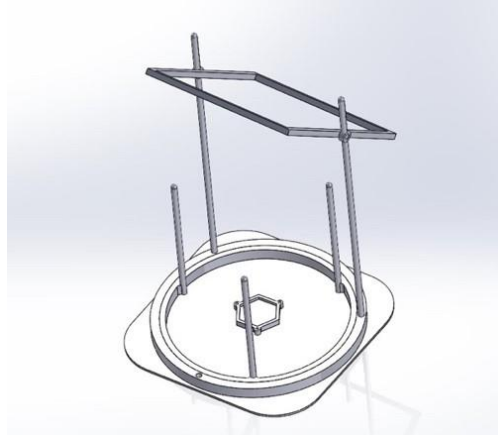


Figure 1: Final Design Assembly

The use of a Fresnel lens capable of sintering lunar regolith to create landing pads was selected for its simplicity, sustainability, and innovative nature. More so, a Fresnel lens is lightweight, power efficient, and will utilize existing lunar materials making for a low-cost barrier for NASA adoption. The sintered tiles will provide enough protection for landers and nearby structures from PSI while also being a multipurposed renewable building material for other lunar applications.

Changes Made Since Proposal

Addressing Tile Grout

NASA feedback addressed an issue that could arise on the moon with the current landing pad design. This was a result from the PISCES Team in Hawaii that found the exhaust from a rocket flowing under the tiles and exploding the landing pad. To solve this issue, the team has discussed and addressing solving it with a rover capable of sintering the grout between each brick. This creates a sealed surface between each tile and does not allow the rocket exhaust to flow underneath.

For this solution to be successful, the rover design must develop a rover capable of traversing the lunar surface with a sintering laser mounted on it. The rover should be equipped with navigation and positioning systems to ensure precise sintering. The sintering laser must use a high-power laser that can effectively sinter the regolith. The laser must be able to create a continuous bond between the tiles and the regolith grout. Preparation of the sintering process is also important. Once the tiles are laid out on the lunar surface with the grout in place, the rover will pass over the seams. After preparation, the laser on the rover will heat the regolith grout and the edges of the tiles, fusing them together. This process will create a solid, continuous surface that prevents exhaust gases from penetrating under the tiles. NASA must ensure this method is safe and tested before implementation. This follows with conducting tests in a simulated lunar environment to refine the sintering process and ensure the bond is strong enough to withstand the conditions of a rocket landing.

In addition, simulate the rocket exhaust impact to verify that the sintered bonds prevent gas penetration and that the tiles remain stable. To further ensure the solution is successful, other considerations must be explored. This includes adding multiple layers of sintering or additional bonding agents to strengthen the grout further and integrating a cooling system to manage the heat generated during the sintering process and ensure even bonding. The overall implementation plan includes Phase 1 of designing and prototyping the tiles and grout material in addition to developing

the rover and sintering laser system. Phase 2 includes conducting laboratory tests to optimize the sintering process and validate the strength of the bonds. Phase 3 includes performing field tests in a lunar analog environment to ensure the system works under realistic conditions. Lastly, Phase 4 includes implementing the design on the lunar surface and monitoring the performance during actual rocket landings.

Addressing Testing in a Vacuum Environment

NASA feedback wanted to make sure that our team knows how the Fresnel Lens set up is going to work in a vacuum environment, presumably because NASA testing with regards to the lunar dust is going to be done in a vacuum environment. Components to address included the Fresnel lens interaction in a vacuum environment, testing set up in a vacuum environment, the impact lower G would have, and any potential problems with creating the tiles that may come up due to a vacuum environment.

Starting with the concern with the Fresnel lens interaction, the sintering of the lunar material can still occur mostly as expected. This is because in a vacuum environment, the mode of heat transfer for the Fresnel lens would be in radiation mode, which combined with no extra heat loss from things like air and other atmospheric components, would allow for sintering of the lunar tiles. It should be noted though that since heat is not being lost through convection due to the lack of atmospheric components, the Fresnel lens would be more efficient in the vacuum chamber than on the actual lunar surface. Understanding these differences is crucial for ensuring that the sintering process is optimized both in the testing phase and during actual lunar operations. By considering the absence of convective heat loss and the enhanced effectiveness of radiative heat transfer, we can better predict and improve the performance of the Fresnel lens system for creating durable lunar tiles.

Addressing Lunar Operations

Additional considerations must be considered for integrating this solution into the greater lunar mission. First, given that the tile production process is time consuming, each time a launch or landing occurs, more lunar ejecta is expelled, and that storage volume is the greatest challenge for transporting this system to the lunar surface, the lens and its accompanying equipment should be brought to the lunar surface on the Starship HLS with the Artemis 3 mission. Then tile production can occur for use with the succeeding Blue Moon HLS.

Operations on the lunar surface can be facilitated with the LTV. Even though payload dimensions of the LTV are not finalized, design of the lunar lens system can be made in conjunction with the rover's specifications, to ensure the cargo storage on the LTV can assist with assembly and moving parts of the lens system to the area of operations. The LTV will also be utilized for collecting lunar regolith, where optimal samples can be gathered and stored in a container for transportation to the lens system, where the container can either integrate directly with the system or can be used alongside it. During production, the tiles can be stacked and stored beside the lens system. Tiles will be picked randomly and will be tested for structural integrity during the manufacturing process to ensure consistent and within-specification production is occurring. Placing the tiles to create the pad can occur in stages, and the LTV can assist with transporting these tiles from the manufacturing location to the landing pad. Lastly, given that the lens system will be static, and materials will be brought to it, the only consideration for the location of the system is its access to continuous sunlight – meaning it can be placed adjacent to the habitat's solar

panel array. This proximity can ensure ongoing research on optimal solar array locations can be utilized with this system, as well as the system can tap into the solar power for operations.

Operations associated with the sintering of the grout between each landing pad tile will require a rover capable of sintering with a 100 W Laser. This is essential to provide the landing pad with no gaps for exhaust from the rockets to damage the landing pad.

Addressing Solar Inclination Angle

One key difference between the environment on the Earth and the south pole of the Moon is that the Lunar south pole has a much shallower solar inclination angle, the max angle being 1.5°. Based on research conducted on the topic, the main concerns with such a scenario are the amount of energy that is reflected off the Fresnel lens and the angle of the test bed needed to perform sintering effectively. Having the Fresnel lens at a steeper angle relative to the horizontal (<45°) allows more energy to transmit through the lens, at the cost of requiring the test bed to sit at a steeper angle (which runs the risk of allowing the lunar regolith to slip out of the bed). Setting the Fresnel lens at a shallower angle gives the reverse outcome, more secure regolith at the cost of more energy reflected off the lens.

An analysis was performed to get a better understanding of how the geometry of different setups would affect the performance of the overall design. To calculate the transmissivity of the Fresnel lens, the following Fresnel equation was utilized:

Equation 1: Transmissivity of Fresnel Lens

$$t_s = \frac{2n_1 \cos \theta_1}{n_1 \cos \theta_1 + n_2 \cos \theta_2}$$

Where n_1 is the refractive index of medium 1, n_2 is the refractive index of medium 2, θ_1 is the angle of the light going from medium 1 (relative to the horizontal), θ_2 is the angle of the light going into medium 2, and t_s is the transmissivity of the lens (the amount of power going through the lens, which is about 1.5° for the Fresnel lens).

The output angles (angles of light going out the front and the back sides of the lens) were calculated from Snell's Law:

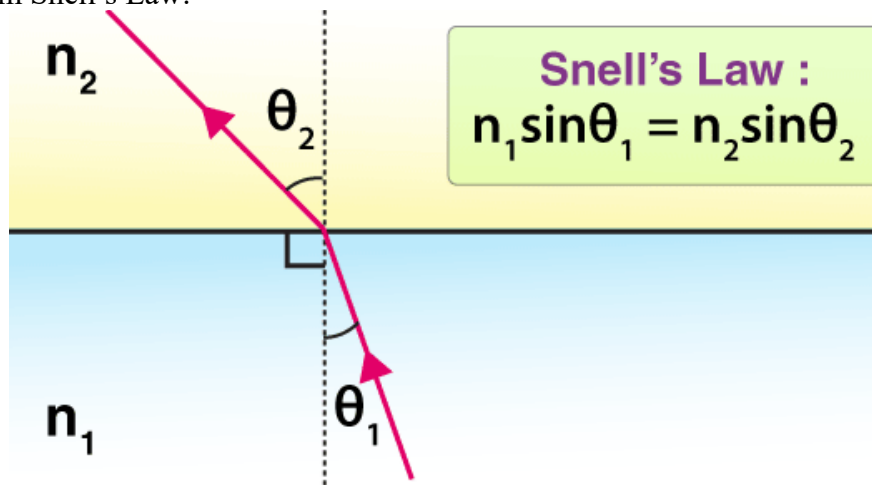


Figure 2: Snell's Law (input/output angles)

Four scenarios were calculated: θ of the lens = 10° , θ of the lens = 30° , and θ of the lens = 45° . For $\theta = 10^\circ$, $t_s = 0.508$ and the angle at which the test bed would be at is 11.5° . For $\theta = 30^\circ$, $t_s = 0.836$ and the angle at which the test bed would be at is 31.5° . For $\theta = 45^\circ$, $t_s = 0.913$ and the angle at which the test bed would be at is 46.5° . There is a diminishing return with increasing the angle of the lens, as can be seen with when $\theta = 60^\circ$. In this scenario, t_s only improved to 0.944 with the angle of the test bed being at 61.5° . Because the angle of repose (angle at which a powder slips) for Apollo 14 regolith samples were found to be around 58° [CM1], it is possible to sinter lunar regolith with design as the Fresnel lens can retain at least 90% of the received power from the Sun.

Addressing Fresnel Lens Material

Further investigation into the material needed for the Fresnel lens was necessary typical acrylic does not have the material properties needed for aerospace applications. Important properties that must be considered are the refractive index, ability to work in hot and cold temperatures, as well as weight for transport. The most plausible material is Polycarbonate which not only has a high refractive index of 1.5848 but is also used in aerospace applications and is proven to handle both hot and cold working temperatures. Finally, the density of Polycarbonate is only slightly higher than that of acrylic (1.20 g/cm³ and 1.18 g/cm³ respectively). The manufacturing of Fresnel lenses out of the chosen material is already established and proven successful for resistance to high impact and temperature fluctuations.

Innovative Technology

The team researched multiple viable solutions but finalized our decision on a Fresnel lens using focused sunlight. This solution has been researched and tested in the past but combining it to be autonomous and for a unique landing pad tile is how our team found to stand out in innovation. In addition, the material of the Fresnel Lens and the angle it focuses sunlight to has been modified to fit our innovative solution. The autonomous design will be able to work along future rover designs and build a landing pad for the NASA Artemis missions within 3-5 years.

Engineering Analysis Fresnel Lens

A Fresnel Lens consists of concentric circles that direct light into a focal point with less material than a traditional converging convex lens. The concentric circles effectively act as a series of convex lenses acting in parallel.

Our proposed design consists of a Fresnel lens measuring 1.016m x 0.762m (40" x 30"). The lens can capture approximately 1400 resulting in a theoretical solar capture of 1.084 kW of power (1.453 hp). The focal area of our lens is 1.267 cm (about 0.5 in diameter: 0.196) at 0.787 m (31 in) from the lens. Our lens has a mass of about 6.35 kg. The lens is made of acrylic with a density of 1.18. Acrylic was chosen due to its thermal properties, low cost, and durability relative to glass and other transparent polymers. This design can be scaled to either increase power output by increasing area or decrease mass for spaceflight by decreasing area. A Pareto front is provided to show corresponding power output relative to lens mass.

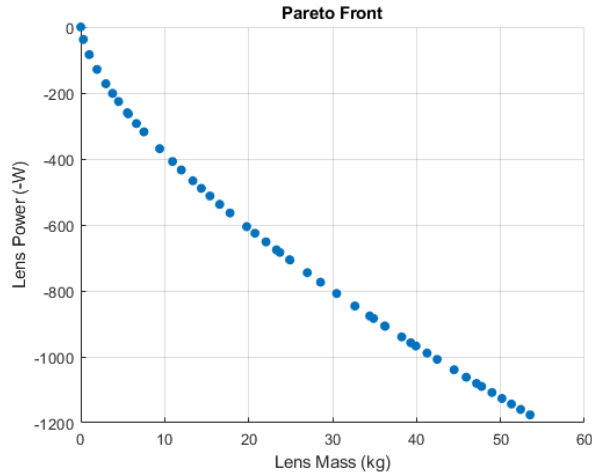


Figure 3: Pareto Front Relating Lens Mass to Negative Lens Power Output

Heat Transfer Calculations

The project team meticulously conducted calculations and analyses about heat transfer and optical considerations. To ensure a comprehensive examination, extensive collaboration took place with esteemed professors from the Mechanical Engineering and Physics departments at Colorado School of Mines, notably with Dr. Rickey Kelly. The outcome of this collaborative effort resulted in the derivation of an equation for determining temperature at various depths over time. The equation assumed a semi-infinite solid under the constant heat flux boundary condition [HT 1]. The derived equation is as follows:

Equation 2: Temperature at various times and depths

$$T(d, t) = \left[\frac{2q''_0 \sqrt{\frac{\alpha t}{\pi}}}{k} \exp\left(-\frac{d^2}{4\alpha t}\right) \right] - \left[\frac{q''_0 d}{k} \operatorname{erfc}\left(\frac{d}{\sqrt{4\alpha t}}\right) \right] + T_i$$

Where T represents temperature, d represents depth from the surface, t represents time, q''_0 represents irradiance, k represents the thermal conductivity of regolith (which is contingent upon the preceding temperature), and alpha represents a ratio derived from the density, conductivity, and volumetric heat capacity of regolith (also dependent on the previous temperature) [HT 2,3,4,5,6]. Additional details regarding these parameters are available in the appendix. A computational program was developed utilizing these equations to estimate sintering phenomena on both lunar surfaces and for testing purposes on Earth. The ensuing results are presented below, and the corresponding source code is accessible in the appendix.

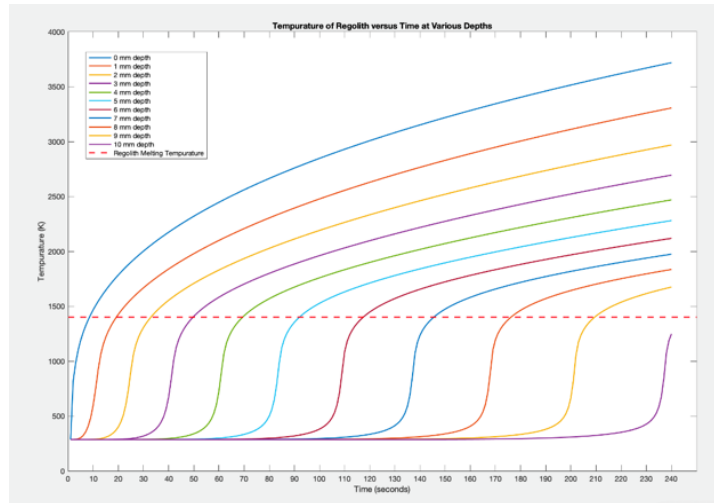


Figure 4: Simulation Graph for Temperature vs. Time

The given graph shows that at a starting temperature of 286 (around 56°F), after four minutes under ideal sintering conditions, nine millimeters in depth will reach the melting point. In testing the model seemed to accurately depict the necessary time and idealization of the system but has limitations about finding various properties for simulated regolith. However, Fresnel lens performance will improve on the moon due to the lack of atmospheric interference.

Electrical Subsystem

The final proposed concept of the device utilizes eight space-rated stepper motors and one fine sun sensor designed for use in space applications. Three motors are used for the rotation of the lens on the z-axis, two motors are used to control the tilt of the lens relative to the lunar surface, and the remaining three motors are used to control the movement of the lunar regolith bed using a system like a delta style 3D printer. The system utilizes three arms connected to the regolith bed attached to three separate vertical rails, these arms move independently of one another along the rails to translate the regolith bed along the x and y axis parallel to the lunar surface. A fine sun sensor positioned on the Fresnel lens is used to track the position and angle of the sun relative to the regolith bed and ensure proper angling of the device throughout operation. All components are space-rated and capable of enduring the harsh lunar environment.

Table 1: Estimated Power Consumption of Required Components [ES3]-[ES5]

Quantity	Component	Voltage	Amperes (A)	Individual Power Consumption (Watts)	Total Power Consumption (Watts)
1	Fine Sun Sensor	5	0.003	0.25	0.25
8	Space-Rated Motor	24	4.2	100.8	806.4
1	Microcontroller	5	5	25	25
1	High-Power Laser	110	90.9	100	100W

Sintering Bed

To optimize strength and ensure proper sintering through the entire material, the idealized system should utilize a sintering bed capable of rotating 360 degrees where two lids contain the regolith between the hexagonal housing. The lids will only open when they are vertical, and gravity is acting against them and will be activated by a cam and follower mechanism and held in place utilizing springs when the lid is not to be open. The lid should open away from the Fresnel lens, and this setup should allow for both sides of the regolith to be sintered. This sintering bed design ensures proper regolith melting throughout the tile and allows for an increased tile thickness at a cost of double the production time.

A Fresnel Lens consists of concentric circles that direct light into a focal point with less material than a traditional converging convex lens. The concentric circles effectively act as a series of convex lenses acting in parallel.

Our proposed design consists of a Fresnel lens measuring 1.016m x 0.762m (40" x 30"). The lens can capture approximately 1400 resulting in a theoretical solar capture of 1.084 kW of power (1.453 hp). The focal area of our lens is 1.267 cm (about 0.5 in diameter: 0.196) at 0.787 m (31 in) from the lens. Our lens has a mass of about 6.35 kg. The lens is made of acrylic with a density of 1.18. Acrylic was chosen due to its thermal properties, low cost, and durability relative to glass and other transparent polymers. This design can be scaled to either increase power output by increasing area or decrease mass for spaceflight by decreasing area. A Pareto front is provided to show corresponding power output relative to lens mass.

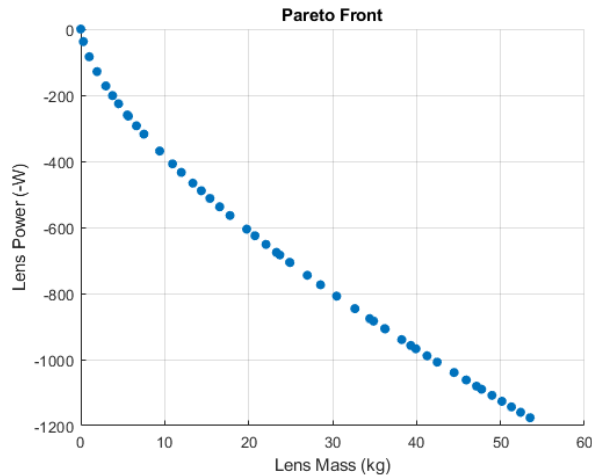


Figure:5 Pareto Front Relating Lens Mass to Negative Lens Power Output

Verification and Validation

The team has designed and built a prototype to test a 43" x 34" Fresnel lens. With current heat transfer calculations, the prototype will sinter regolith simulant to a depth of 1cm (about 0.39 in) in 4 minutes. This will require a flux of $5.3266 \times 10^4 \left[\frac{W}{m^2} \right]$ from the lens which will reach a temperature of $2000^\circ F$ on the regolith simulant surface. Using this data and test results, our team has verified the prototype and determined the heat transfer calculations on the moon to be reliable. Further validation testing needs to be done considering the Earth environment where testing was done has external factors such as wind which adds additional convection, reducing the efficiency of the Earth based test system. Moreso, the Earth atmosphere scatters radiation, however on the

moon, the lack of atmospheric interference will also add to the efficiency of a theoretical lunar based sintering system.



Figure:6 Testing of Fresnel Lens

Conclusion

The Prudent Landers were successful this past year with implementing the Fresnel lens into an autonomous design and allowing NASA to mitigate plume effect damages in the future through a landing pad process. After the Prudent Landers successfully tested a Fresnel lens in Denver Colorado with regolith simulant, the expected results matched the testing results and validated the calculations made for use on the South Pole of the Moon. The team addressed the project proposal feedback and improved the design and systems approach for the device to function. The Prudent Landers are excited to present the project as it can further be used for not just landing pad tiles, but any other nature of utilizing sintered regolith into any shape or part. The design and systems approach of operations allows limited risk due to the autonomous device and a controlled focal point with concentrated solar energy. Human interaction is required to lay the tiles with the LTV used as a transportation vehicle of the landing pad tiles

Path-To-Flight Timeline

The targeted solution aims to be flight ready by 2027 or early 2028. Following a standard NASA product lifecycle, Figure 6 details the project phases from formulation to implementation adapted to capture the targeted launch date of 2027 [P2F 1]. This timeline assumes most of the Pre-Phase A, Concept Studies, is already captured in this report. Technology development and preliminary designs will also be straightforward, estimated seven months, as a solar lens and 3-D printer technology is widely available and well documented. After preliminary approval, fabrication, assembly, integration, and launch have wide margins, respectively. These margins consider the legitimate engineering effort that needs to go into human lunar landing. Therefore, to minimize crew risk, extra precautions should be taken into integration and testing to ensure a reliable product.

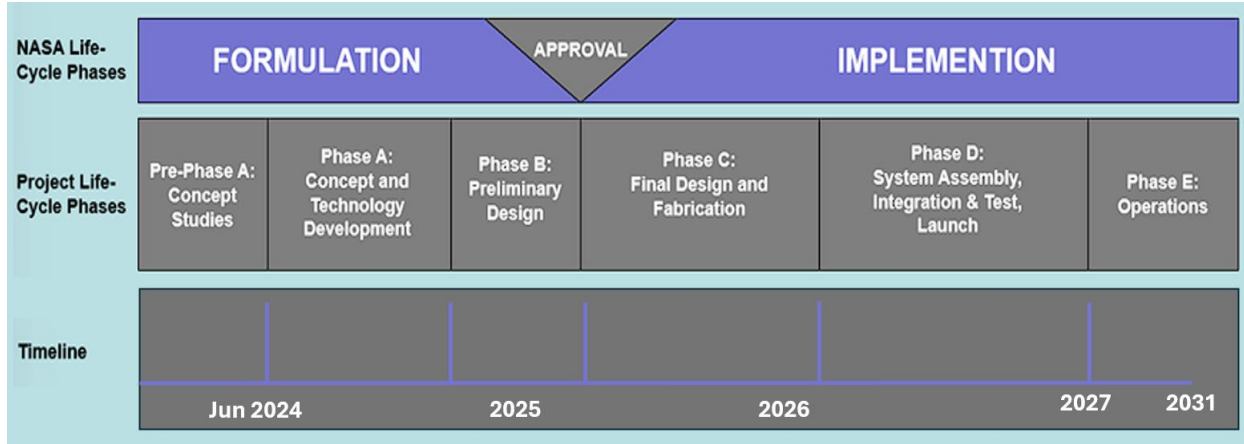


Figure 7 Path-to-Flight Timeline

Cost Estimation

Budget estimations were done using NASA’s Cost Estimation Toolkit (CET) under the following assumptions. Firstly, the mission will start in 2024 and production will last three years to align with HuCL implementation guidelines. Moreover, mission operations are assumed to last an additional five years. Labor estimations through CET used the following positions and average salaries: Senior Aerospace Engineer (\$110k-\$175k) [CE1], Systems Engineer (\$64k-\$138k) [CE2], Project Engineering Manager (\$117k-\$193k) [CE3], Software Engineer (\$74k-\$191k) [CE4], CAD Designer (\$41k-\$107k) [CE5], Electrical Engineer (\$74k-\$191k) [CE6], Industrial Engineer (\$89k-\$133k) [CE7], and Mechanical Technician (\$44k-\$100k) [CE8]. Yearly budgets of \$25,000 were allocated to software maintenance, travel, and facility preparation and support costs.

Figure 7 (below) shows projected cost estimations from CET. Over a period from 2024 to 2031, an estimated total cost of \$2,430k was projected for the entire program. Two thirds of the budget is predicted to account for labor costs and leaving the remaining third to be used for non-staff costing including materials and facilities.

Life Cycle Cost Estimate		Activity Dataset: HuCL							Produced: 06/04/24							
Mission Start Year:	2024	Operations Start Year:				2027	Mission Complete Year:				2031	Inflation Rate		3.0%		
Estimated Staffing Level	2024	2025	2026	2027	2028	2029	2030	2031	2032	2033	2034	2035	Total	Pct.		
Management Staff FTE	0.25	0.25	0.25	0.50	0.50	0.50	0.50	0.50	0.00	0.00	0.00	0.00	3.25	27.3%		
Administrative Support FTE	0.00	0.00	0.00	0.02	0.02	0.02	0.02	0.02	0.00	0.00	0.00	0.00	0.10	0.8%		
Technical Coordination Staff FTE	0.00	0.00	0.00	0.75	0.75	0.75	0.75	0.75	0.00	0.00	0.00	0.00	3.75	31.5%		
Development Staff FTE	0.01	0.01	0.01	0.00	0.00	0.00	0.00	0.00	0.00	0.00	0.00	0.00	0.03	0.3%		
Technical / Science Staff FTE	0.00	0.00	0.00	0.00	0.00	0.00	0.00	0.00	0.00	0.00	0.00	0.00	0.00	0.0%		
Operations Staff FTE	0.00	0.00	0.00	0.08	0.08	0.08	0.08	0.08	0.00	0.00	0.00	0.00	0.38	3.2%		
Sustaining Engineering Staff FTE	0.00	0.00	0.00	0.06	0.06	0.06	0.06	0.06	0.00	0.00	0.00	0.00	0.28	2.3%		
Engineering Support Staff FTE	0.00	0.00	0.00	0.83	0.83	0.83	0.83	0.83	0.00	0.00	0.00	0.00	4.13	34.6%		
Estimated Total FTE	0.26	0.26	0.26	2.23	2.23	2.23	2.23	2.23	0.00	0.00	0.00	0.00	11.92			
Estimated Staff Costs, K\$	2024	2025	2026	2027	2028	2029	2030	2031	2032	2033	2034	2035	Total	Pct.		
Management Staff Cost	38	39	40	82	84	87	90	92	0	0	0	0	551	35.5%		
Administrative Support Staff Cost	0	0	0	1	1	1	1	1	0	0	0	0	7	0.4%		
Technical Coordination Staff Cost	0	0	0	82	84	87	90	92	0	0	0	0	435	28.1%		
Development Staff Cost	1	1	1	0	0	0	0	0	0	0	0	0	4	0.2%		
Technical / Science Staff Cost	0	0	0	0	0	0	0	0	0	0	0	0	0	0.0%		
Operations Staff Cost	0	0	0	8	9	9	9	9	0	0	0	0	45	2.9%		
Sustaining Engineering Staff Cost	0	0	0	6	6	6	7	7	0	0	0	0	32	2.1%		
Engineering Support Staff Cost	0	0	0	90	93	96	99	101	0	0	0	0	479	30.9%		
Total Estimated Staff Cost	39	40	41	269	277	286	296	302	0	0	0	0	1,550	63.8%		
Other Non-Staff Costs	2024	2025	2026	2027	2028	2029	2030	2031	2032	2033	2034	2035	Total	Pct.		
System Purchase Cost	2	2	2	0	0	0	0	0	0	0	0	0	6	0.7%		
COTS Software License Cost	7	7	7	3	3	3	3	3	0	0	0	0	36	4.1%		
Facility Preparation and Support Cost	23	23	23	33	33	33	33	33	0	0	0	0	234	26.6%		
System Maintenance Cost	0	0	0	4	4	4	4	4	0	0	0	0	20	2.3%		
Network / Communications Cost	4	4	4	4	4	4	4	4	0	0	0	0	32	3.6%		
General Supplies Cost	10	10	10	13	13	13	13	13	0	0	0	0	95	10.8%		
Archive Media Cost	0	0	0	0	0	0	0	0	0	0	0	0	0	0.0%		
Distribution Media Cost	0	0	0	0	0	0	0	0	0	0	0	0	0	0.0%		
Travel Cost	25	25	25	25	25	25	25	25	0	0	0	0	200	22.7%		
Training Cost	0	0	0	3	1	1	1	1	0	0	0	0	7	0.8%		
Data Purchase Cost	0	0	0	25	25	25	25	25	0	0	0	0	125	14.2%		
Computer Services Cost	0	0	0	25	25	25	25	25	0	0	0	0	125	14.2%		
Total Estimated Non-Staff Costs, K\$	71	71	71	135	133	133	133	133	0	0	0	0	880	36.2%		
Total Estimated Cost, K\$	110	111	112	404	410	419	429	435	0	0	0	0	2,430			

Figure:8 Project Cost Timeline

I. Appendix One – Heat Transfer Calculations:

$T_i = 286 [K](\sim 56^\circ F)$, or previous second's T value at a given depth

$$q_o'' = 5.3266 * 10^4 \left[\frac{W}{m^2} \right] [HT2, 3]$$

Equation 3: Irradiation/Solar Flux (constant)

$$k = (1.281 * 10^{-2}) + (4.431 * 10^{-10})(T_i) \left[\frac{W}{m*K} \right] [HT4]$$

Equation 4: Thermal Conductivity of Regolith

$$\rho = 1500 \left[\frac{kg}{m^3} \right] [HT4]$$

Equation 5: Density of Regolith (constant)

$$C_p = (-3.6125) + (2.7431)(T_i) + (2.3626 * 10^{-3})(T_i^2) - (1.234 * 10^5)(T_i^3) + (8.9093 * 10^{-9})(T_i^4) \left[\frac{J}{kg*K} \right] [HT5]$$

Equation 6: Volumetric Heat Capacity of Regolith

$$\alpha = \frac{k}{\rho * C_p} [No units] [HT1]$$

Equation 7: Alpha Ratio


```

1  %% SECTION ONE: initialize variables
2  clc; clear all; close all
3
4  %Below values and equations will be used if specific location values are unknown or not given:
5  T_i = 0; % [K] location initial temp
6  T_melt = 1400; % [K] regolith melting temp
7  k = @(T_n) (1.281*(10^-2)) + (4.433*(10^-10))*(T_n^3); % Conductivity due to previous temp
8  cp = @(T_n) (0.25+(2.7*(10^-4)*T_n)+(2.36*(10^-6)*T_n^2)-(1.2*(10^-8)*T_n^3)+(8.809*(10^-10)*T_n^4)); %capacity due to previous temp
9  rho = 1500; % [kg/m^3] Density of Packed Regolith
10 T_max = 0; % maximum runtime of lens
11 d_max = 0; % maximum depth location
12 T = zeros; %table of temperatures
13
14 %% SECTION TWO: user select location and regolith
15 [indxL,tf] = listdlg('PromptString', {'Select Location'}, 'SelectionMode', 'single',...
16 'ListSize', [150,100], 'ListString', {'Earth', 'Moon'});
17
18 if (indxL == 1) %Earth
19     fprintf('Location: Earth\n');
20     T_i = 286; % [K]
21
22     %user input(regolith type)
23     [indxR,tf] = listdlg('PromptString', {'Select Regolith Simulant Type'}, 'SelectionMode', 'single',...
24 'ListSize', [150,100], 'ListString', {'TUBS-T', 'TUBS-M'});
25     if (indxR == 1) %TUBS-T
26         fprintf('Regolith: Simulant TUBS-T\n');
27         T_melt = 1972; % [K]
28         k = @(T_n) 9.7*(10^-4); % [W/(mK)]
29         cp = @(T_n) 548; % [J/(kgK)]
30         rho = 1400; % [kg/m^3]
31     elseif (indxR == 2) %TUBS-M
32         fprintf('Regolith: Simulant TUBS-M\n');
33         T_melt = 1523; % [K]
34         k = @(T_n) 1.2*(10^-3); % [W/(mK)]
35         cp = @(T_n) 551; % [J/(kgK)]
36         rho = 1400; % [kg/m^3]
37     else
38         fprintf('Error: Regolith selection Invalid\n');
39     end
40
41 elseif (indxL == 2) %Moon
42     fprintf('Location: Moon\n');
43     T_i = 250; % [K]
44
45     %user input(regolith type)
46     [indxR,tf] = listdlg('PromptString', {'Select Regolith properties based on location'}, 'SelectionMode', 'single',...
47 'ListSize', [150,150], 'ListString', {'South Pole', 'Apollo Landing', 'General Properties'});
48     if (indxR == 1) %South Pole
49         fprintf('Regolith: South Pole\n');
50         T_melt = ? % [K]
51         k = @(T_n) 0.401; % [W/(mK)]
52         cp = @(T_n) ? % [J/(kgK)]
53         rho = 2370; % [kg/m^3]
54     elseif (indxR == 2) %Apollo Landing
55         fprintf('Regolith: Apollo Landing\n');
56         T_melt = 1500; % [K]
57         k = @(T_n) 0.8008; % [W/(mK)]
58         cp = @(T_n) 524; % [J/(kgK)]
59         rho = 1756; % [kg/m^3]
60     elseif (indxR == 3) %General Properties
61         fprintf('Regolith: General Properties\n');
62         T_melt = 1400; % [K]
63         k = @(T_n) ? % [W/(mK)]
64         cp = @(T_n) ? % [J/(kgK)]
65         rho = ? % [kg/m^3]
66     else
67         fprintf('Error: Regolith selection Invalid\n');
68     end
69
70 else
71     fprintf('Error: Location selection Invalid\n');
72 end
73
74 %% SECTION THREE: user input for lens specs
75 %user input(lens something) width? density? Mass? angle?
76 prompt = {'Diameter [m]', 'Internal Angle [degrees]', 'Focal Length [m]'};
77 dlgtitle = 'Fresnel Lens Specification (changes flux)';
78 fieldsize = [1 50; 1 50; 1 50];
79 definput = {'1', '10', '%'};
80 answer1 = inputdlg(prompt, dlgtitle, fieldsize, definput);
81 q_s = 4.06*(10^6); % [W/m^2] Solar Flux based on Fresnel Lens << I DONT KNOW HOW TO CHANGE THIS !!!
82
83 %% SECTION FOUR: user input for depth and time
84 prompt = {'Maximum Time [seconds]', 'Maximum Depth [m]'};
85 dlgtitle = 'Define Scope of Study';
86 fieldsize = [1 50; 1 50];
87 definput = {'200', '0.01'};
88 answers = inputdlg(prompt, dlgtitle, fieldsize, definput);
89
90 t_max = str2double(answers{1}); %max "run time" of system
91 time_t = [1:t_max, 1]; % [s] Table of times counting up by seconds
92
93 d_max = str2double(answers{2}); % maximum depth (in meters)
94 depth = [0:d_max/30:d_max]; % [m] Table of depths counting up by mms
95
96 %% VERIFICATION: output values to user
97 T_n = T_i;
98 fprintf('Initial Values: Initial Temp: %d [K] \n Melting Temp: %d [K] \n Conductivity: %d [W/(mK)] \n T_i: %d, k(T_i):', T_i, T_melt, k(T_i))
99 fprintf('\n Capacity: %d [J/(kgK)] \n Density: %d [kg/m^3] \n Maximum Time: %d [s] \n Maximum depth: %d [m] \n', cp(T_i), rho, t_max, d_max)
100
101 %% SECTION FIVE: fill temperature table
102 for d = 1:11 %setting initial temperature for all depths to 286K
103     T(i,d) = T_i;
104 end
105
106 for t = 2:t_max %loop through all times
107     for d = 1:11 %loop through all depths
108         T_n = T(i-1,d); %Variable is the temperature in the previous second, at that depth, used for calculations
109         k_n = k(T_n);
110         cp_n = cp(T_n);
111         alpha = k_n/(rho*cp_n);
112         T(i,d) = ((2*(k_n*(1+(alpha*time_t(i)/d)))^(1/2)/d) + (exp(-(depth(d)^2)/(4*(alpha*time_t(i)))))) - ((q_s*depth(d))/k_n + ...
113             (erfc(depth(d)/(2*(sqrt(alpha*time_t(i)))))) + T_n; %Temperature of this time at this depth
114     end
115 end
116
117 %% SECTION SIX: plot results
118
119 plot(T, 'Linewidth', 1.5) % plot found data
120 title('Temperature of Regolith versus Time at Various Depths')
121 xlabel('Time (seconds)')
122 xticks(0:10:t_max)
123 ylabel('Temperature (K)')
124 hold on
125
126 h = yline(T_melt, 'r--', 'Linewidth', 2); %plot melting temperature asotope
127
128 Lnames = string(depth + 100) + 'm'; %Labeling Legend
129 legend(Lnames(1), Lnames(2), Lnames(3), Lnames(4), Lnames(5), Lnames(6), Lnames(7), Lnames(8), Lnames(9), Lnames(10), 'Regolith Melting Temperature')...
130 'Location', 'best')
131

```

Figure:9 Source Code for Heat Transfer Calculations

II. Appendix Two- References

[CM1] C. I. Calle and C. R. Buhler, "Measurement of the angle of repose of apollo 14 lunar sample 14163.," *The Impact of Lunar Dust on Human Exploration*, no. 2141, p. 5030, Feb.2020.

[ES1]Ginés-Palomares, JC., Fateri, M., Kalhöfer, E. et al. Laser melting manufacturing of large elements of lunar regolith simulant for paving on the Moon. *Sci Rep* 13, 15593 (2023). <https://doi.org/10.1038/s41598-023-42008-1>

[ES2] C. Q. C. published, "Scientists want to make moon roads by blasting lunar soil with sunlight," *Space.com*, Oct. 16, 2023. <https://www.space.com/blasting-lunar-soil-with-sunlight-could-create-moon-roads#:~:text=%22Tiles%20could%20be%20created%20on.>

[HT1] T.L. Bergman, and A.S. Lavine, *Fundamentals of Heat and Mass Transfer*, 8th edition, Wiley, 2017.

[HT2] Zhang, K.; Su, Y.; Wang, H.; Wang, K.; Song, J, "Highly Concentrated Solar Flux of Large Fresnel Lens Using CCD Camera-Based Method," *Sustainability*, 2022.

[HT3] D. Williams, "Moon Fact Sheet," *NASA.gov*, 2017.

[HT4] Colozza, A., "Analysis of Lunar Regolith Thermal Energy Storage," Brook Park, Ohio: *Lewis Research Center Group*, 1991.

[HT5] Austen D.H., Shafirovich E., "Specific Heats and Thermal Diffusivities of LHS-1 Lunar Regolith Simulant at Low Temperatures," El Paso, TX: *Department of Aerospace and Mechanical Engineering, The University of Texas at El Paso*, 2023.

[HT6] Kost P.M., Linke S., Gundlach B., Lethullier A., Baasch J., Stoll E., Blum J., "Thermal Properties of Lunar Regolith Simulant Melting Specimen," Vol. 187: *Acta Astronautica*, 2021.

[P2F 1] "SEH 3.0 NASA Program/Project Life Cycle - NASA." <https://www.nasa.gov/reference/3-0-nasa-program-project-life-cycle/>

[ES3] R. P. Ltd, "Raspberry Pi 5," *Raspberry Pi*. <https://www.raspberrypi.com/products/raspberry-pi-5/>

[ES4] Bradford Space, "Fine Sun Sensor," QD74CQ datasheet, Jan. 2017. <https://satsearch.co/products/bradford-fine-sun-sensor/>

[ES5] *American-motion.com*, 2023. <https://american-motion.com/space/products/hybrid-stepper-motors/nema-23/V5718L-A10P/>

[ES6] K. W. Farries, P. Visintin, and S. T. Smith, “Direct laser sintering for lunar dust control: An experimental study of the effect of simulant mineralogy and process parameters on product strength and scalability,” *ScienceDirect*, 2022.

[CE1] “Senior Aerospace Engineer Salary in USA - Average Salary,” *Talent.com*. <https://www.talent.com/salary?job=senior+aerospace+engineer>.

[CE2] “System Engineer Salary in North Carolina”, *Indeed*. <https://www.indeed.com/career/system-engineer/salaries/NC>

[CE3] Salary.com, “Project Engineering Manager Salary,” *Salary.com*. <https://www.salary.com/research/salary/benchmark/project-engineering-manager-salary>

[CE4] Indeed, “How Much Does A Software Engineer Make In United States?,” *www.indeed.com*, 2023. <https://www.indeed.com/career/software-engineer/salaries>

[CE5] Indeed, “CAD Designer Salary in United States,” *www.indeed.com*, 2023. <https://www.indeed.com/career/cad-designer/salaries>

[CE6] Indeed, “Software Engineer Salary in United States,” *www.indeed.com*, 2023. <https://www.indeed.com/career/software-engineer/salaries>

[CE7] Salary.com, “Senior Industrial Engineer Salary in the United States”, *Salary.com*, 2023. <https://www.salary.com/research/salary/alternate/senior-industrial-engineer-salary>.

[CE8] Payscale, “Average Mechanical Technician Hourly Pay,” *Payscale*, 2023. https://www.payscale.com/research/US/Job=Mechanical_Technician/Hourly_Rate

[CE9] “Cost of space launches to low Earth orbit,” *Our World in Data*, 2023. <https://ourworldindata.org/grapher/cost-space-launches-low-earth-orbit>